Geochemical Modeling and Hydrocarbon Generation Potentiality of Source Rocks of the Oligocene to Miocene Succession in the Temsah Area, Eastern Nile Delta, Egypt

Mohamed S. Fagelnour[1], Amr Talaat[2], Amir Ismail[3], Abdelrahman S. Gad[3] and Nader A. Edress[3,*]

[1]   Khalda Oil Company, Cairo, Egypt
[2]   Belayim Petroleum Oil Company, Cairo, Egypt
[3]   Geology Department, Faculty of Sciences, Helwan University, Cairo, Egypt
*   **Correspondence**: nedress@science.helwan.edu.eg ; nedress@outlook.com

Abstract

Geochemical investigation of the Temsah-4 well (T-4) in Temsah gas fields at the eastern offshore Nile Delta differentiate into two categories of OM (organic matter) which are kerogen types II and III within the boreholes penetrated Oligocene-Miocene source rocks. The geochemical and lithological characteristics of the OM-bearing formations in the investigated borehole recognized four thick organic matter-rich intervals (OMRI) in well T-4. The OMRI considers a part of formations that are believed to be considered a real source rock that comprises approximately 66.68% of the Wakar, 65.17% of Sidi-Salem, and 100% of Qantara Fms in the T-4 well. They comprised intervals depths of 3120m-3150m and 3300m-3559.4m belonging to Wakar Fm, from 3580m- 3870m belonging to Sidi-Salem Fm and from 3977m- 4170m belonging to Qantara Fm. The geochemical data reveals that Wakar Fm in the T-4 well considers immature source rock. While mature OMRI within Sidi-Salem and Qantara Fms in the T-4 well represented as effective mature source rocks. Construction of a TOC map in two dimensions throughout the studied areas shows a trend of increasing the quantity of OM eastward during the deposition of Sidi-Salem and Wakar Fms. The improvements of the richness (relatively high TOC) toward the eastward suggested a favorable condition for preservation and accumulation of OM toward the east than the west drilled boreholes. Based on the relative hydrocarbon potential (RHP) the suggested expulsion threshold depths appear to be shallower at 3700m in T-4. Burial history diagrams of studied T-4 wells based on geochemical results postulate that Tineh Fm enters the early mature stage at 2.8Ma. The maturity continues till the recent periods to enter the Qantara and most of Sidi-Salem Fms the same main-oil window at the T-4 area.

Keywords: Temsah gas field; Source rock; Organic matter rich intervals; Expulsion threshold Depth; Maturity

1. Introduction

The proven gas reserves of Egypt equal 98 trillion cubic feet and 18.5 billion barrels of oil and condensate as of the end of 2016. Exploration activity continues to add new giant gas discoveries, particularly in the offshore Nile Delta and Mediterranean (Dolson, 2020). The Plio-Pleistocene to Miocene siliciclastic reservoirs in the Nile Delta and offshore Mediterranean Sea basins have produced natural gas. These provinces have the highest growth and exploration levels in Egypt. The recent decade's large Pliocene gas discoveries confirmed the interval as the main hydrocarbon target for

development in the Nile Delta and the offshore Mediterranean. The area of study includes Temsah (T) and Temsah-North-West (T-NW) gas fields in the Temsah concession in the Eastern Mediterranean and offshore of the Nile Delta of Egypt. It is about 65 Km north to northwest of Port said between latitudes 31°48"N, and 31°53"N, and longitudes 32°04"E, and 32°12"E (Fig.1). The Temsah Field contains 4-7 trillion cubic feet in its structure (Dolson, 2016).
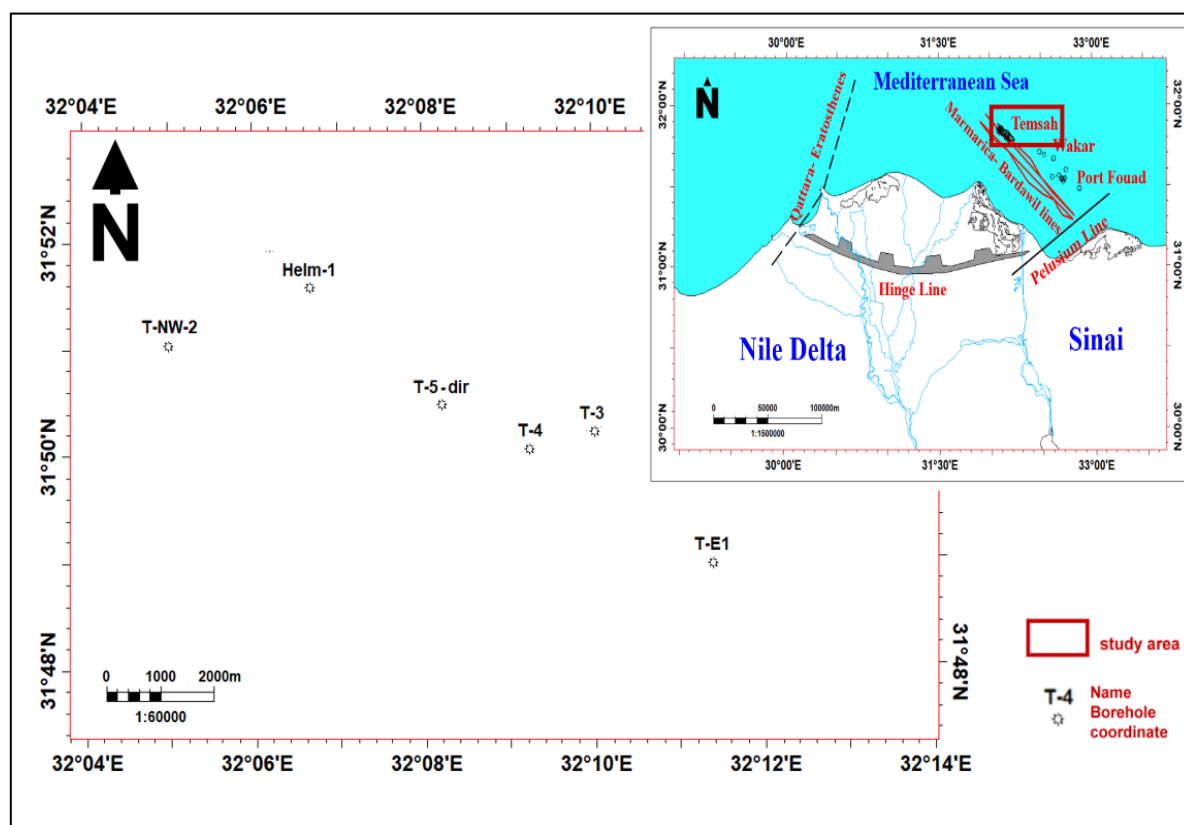

Fig.1. location of the study area and regional tectonic setting of Nile Delta (Schlumberger, 1995)

The Nile Delta and East Mediterranean are mostly known as natural gas-prone provinces with gas and condensate production from the Miocene and Pliocene fields (Shaaban et al., 2006, Ismail et al., 2020b and 2022). Mesozoic reservoirs are present at greater depth and have been penetrated by a few wells which are located in the south delta block. Source rocks are present in the Kafr El-Sheikh and Sidi-Salem formations. The Triassic and (Neocomian) organic-rich shales are proven to be effective oil source rocks, while Jurassic carbonates and Oligocene shales are potential gas-prone source rocks (Schlumberger, 1984). The shales of Sidi Salem, Wakar, and Kafr El Sheikh formations are considered fair to very good source rocks, while the thin sandstone alternated lamina are good for considering reservoir rocks (Khaled et al., 2014). The upper Miocene depositional system appears to be the most effective target in the East Mediterranean area because it contains a broad range of depositional environments, such as fluvial, shallow marine reservoirs, and/or deep-water turbidity sands (Abdel Aal et al., 2000).

The general scope of the present research is giving a general aspect of the Temsah and Temsah-NW gas-fields from the petroleum exploration viewpoints based on the geochemical analysis and well-logging interpretations of six boreholes in the studied areas (T-3, T-4, T-5, T-E1 of Temsah and Helm-1, T-NW-2 of Temsah-NW). To accomplish the previous goals, the present study dealing with the

following concept of; a) participating in the well-logging data for determining the TOC (from LLD-deep resistivity and sonic logs) in wells which lack geochemical data; b) identify the lithology of sedimentary sequence penetrated the studied wells (from well-logging and composite mud-logs column); c) calculate and interpret a geochemical Rock-eval measured parameters (from collected ditch-samples of one T-4 well) and d) evaluate the potentiality of the main source rocks of Wakar, Sidi-Salem, Qantara, and Tineh Fms according to their quantity, quality and maturity that responsibly producing the HC in the present gas-field by applying OMRI method steps according to of Edress et al. (2021).

Moreover, the authors used methods of Pang et al. (2019) and Edress et al. (2021 and 2022) to predict both the expulsion threshold and ASDL depths in the two areas according to relative hydrocarbon potential (RHP). The timing of the beginning of the HC generated is mentioned also according to burial history modeling in the two investigated areas. Furthermore, structure contour maps for the three top of the OM-bearing formations (Qantara, Sidi-Salem and Wakar Fms) are used to spotlight the closure areas for more acceptable HC entrapment sites in the present field.

2. Geological Setting

The Nile Delta Basin occupies more than 250,000 km2 in the eastern Mediterranean province (Kirschbaum et al., 2010) which is divided into western, eastern, and central sub-basins (Bertello et al., 1996; Marten et al., 2004; Nabawy and Shehata, 2015). The Nile Delta and its offshore extension into the Mediterranean was affected by a four major structural alignments (Said, 1990; Schlumberger 1995). These tectonic trends are the two northwest-southeast trending Marmarica and Bardawil (Temsah) lines, and the northeast-southwest trending Qattara and Eratosthenes and Pelusium lines (Fig.2). The two northwest-trending lines played an important role in forming the Neo-Tethys Ocean in the Jurassic time. The Early Jurassic rifting, associated with the breakup of Pangea, made the deep NE-SW and some E-W trending basins in the Western Desert of Egypt (Dolson, 2020). These rift basins extend to involve the Nile Delta cone and the Levant basin in the East Mediterranean. It is uncertain what the contribution of the deep Jurassic and Cretaceous source rocks might have HC in the Nile Delta and the East Mediterranean. Another significant geological feature is the Hinge Line, which indicates the southern limit of the rifted continental margin of northern Egypt. Its origin dated back to the Jurassic crustal break-up of the southern Neo-Tethys (Said, 1990). WNW to ESW faults split the delta into two sub-provinces. The faulted flexure divides the south delta province and the north delta basin. Four reactivated fault systems the Bardawil Line, Qattara-Eratosthenes Line, Pelusium Line, and Hinge Zone controlled the northern deltas. The Hinge Line marks the abrupt transition from the continental facies and unconformities to the south and the deep-water Oligo- Miocene turbidites to the north. The Oligocene to Early Miocene sediments are well developed north to the Hinge Line which is marked by strong subsidence and deposition in a marine environment (Fig.2). These sediments constitute the Tineh Formation (Oligocene) and Qantara Formation (Early Miocene), with an unconformity between them (Bertello et al., 1996; El-Heiny and Enany, 1996). Diapers, overthrust faults, and asymmetric folds are some of the geological features that define the Nile Delta. Its origins can be traced back to the Syrian Arc system, which followed an arcuate path from the northeast to the southwest, crossing through the northern portion of the Nile Delta and terminating in Egypt's Western Desert (Hemdan et al., 2002).
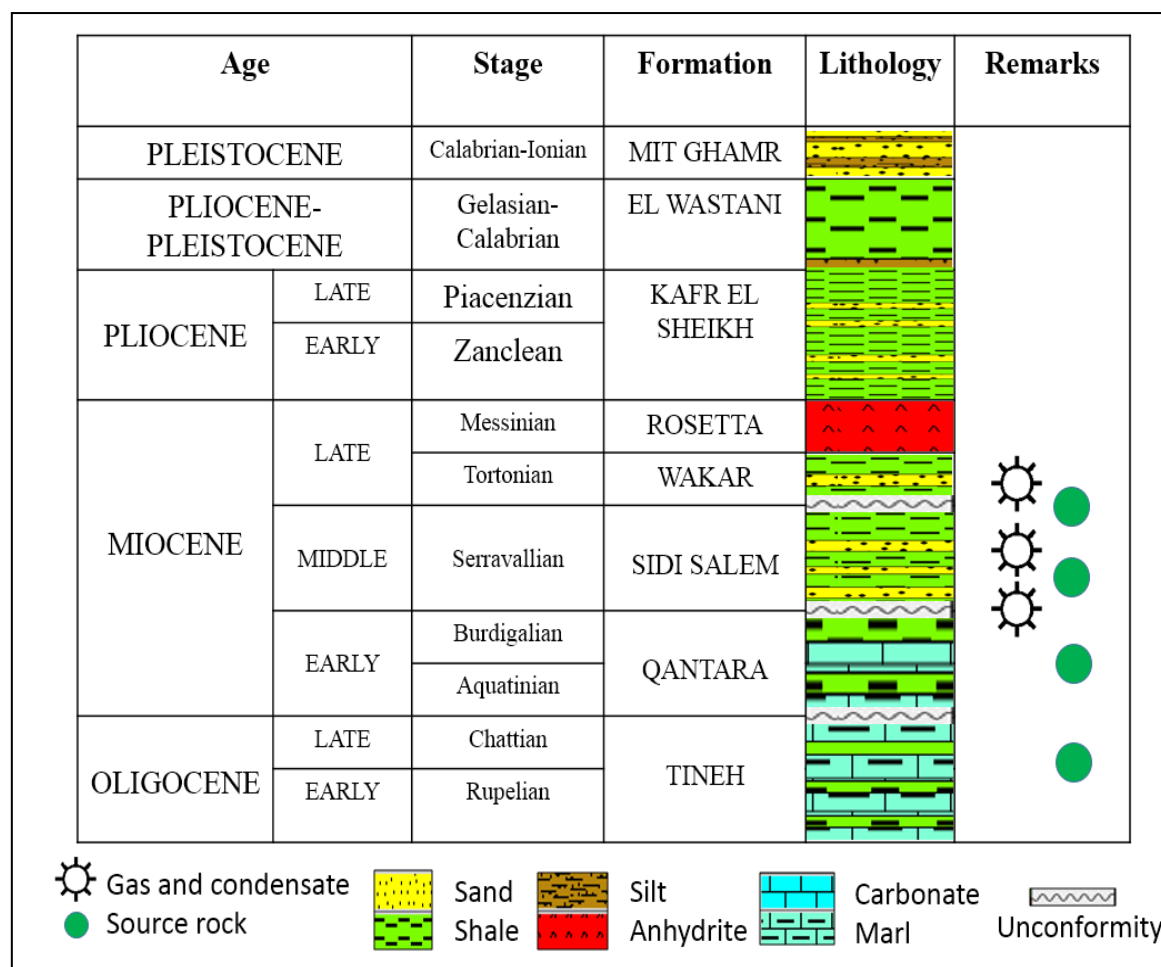
Age		Stage	Formation	Lithology	Remarks
PLEISTOCENE		Calabrian-Ionian	MIT GHAMR		
PLIOCENE-PLEISTOCENE		Gelasian-Calabrian	EL WASTANI		
PLIOCENE	LATE	Piacenzian	KAFR EL SHEIKH		
	EARLY	Zanclean			
MIOCENE	LATE	Messinian	ROSETTA		
		Tortonian	WAKAR		☼ ●
	MIDDLE	Serravallian	SIDI SALEM		☼ ● ☼ ● ☼
	EARLY	Burdigalian	QANTARA		●
		Aquatinian			
OLIGOCENE	LATE	Chattian	TINEH		●
	EARLY	Rupelian			

☼ Gas and condensate   ● Source rock   ▒ Sand   ▒ Shale   ▒ Silt   ▲ Anhydrite   ▒ Carbonate   ▒ Marl   〰 Unconformity

Fig.2. The stratigraphic succession of the Eastern offshore Nile-Delta and East Mediterranean (Younes, 2015; Edress et al., 2022; El-Moghazy et al., 2023)

In general, the stratigraphy of the Nile Delta and East Mediterranean concessions is quite similar as shown in Fig. 2, summarized by different authors of Said (1990), Khaled et al. (2014), Lashin and Abd El-Aal, (2005), Shaaban et al. (2006), Dolson (2020), Ismail et al. (2020) and Edress et al. (2022), El-Moghazy et al. (2023) as following events. An wide marine transgression that covered the Nile Delta occurred in the Aquatinian- Burdigalian Time and led to the deposition of thick marls and shales of the Qantara Formation. During the latest Burdigalian to Langhian time, the Arabia/Eurasia convergence plates boundaries led to positive highlands, which subsequent to a strong erosion of the exposed formations. During Serravallian a high subsidence and the deposition of thick terrigenous sediments of the Sidi-Salem Fm. From south to north, transitional to shallow marine deposits gradually pass to finer sand and shale prograding complex. The Serravallian turbiditic sandy systems of the Sidi Salem Formation were deposited at least in the Temsah and Wakar fields (Bertello et al., 1996). A strong erosive event occurred at the end of Serravallian due to a new series of positive movements and caused the Serravallian/Tortonian unconformity which was recorded over all the area (El-Heiny and Enany, 1996). The Tortonian Wakar Formation is represented by a turbidity complex deposited in frontal areas. About 8 million years ago, a regional sea level drawdown with 550 m of sea level lowering occurred. It is thought to be due to the closure of the straits of Gibraltar, which created the Messinian crisis. Widespread salts and evaporites were deposited in the Mediterranean Basin (Pigott et al., 2014; Leila and Moscariello, 2018). Pliocene delta progradation made the youngest traps and reservoirs in the Nile

Delta and Mediterranean (Dolson, 2020; Ismail et al., 2021). A wide transgression occurred at the beginning of Pliocene Time and led to the deposition of thick marine sequences, favored by the gradual sinking of the Mediterranean where Kafr El-Sheik, El Wastani, and Mit Ghamr formations were deposited (Said, 1990) (Fig. 3).
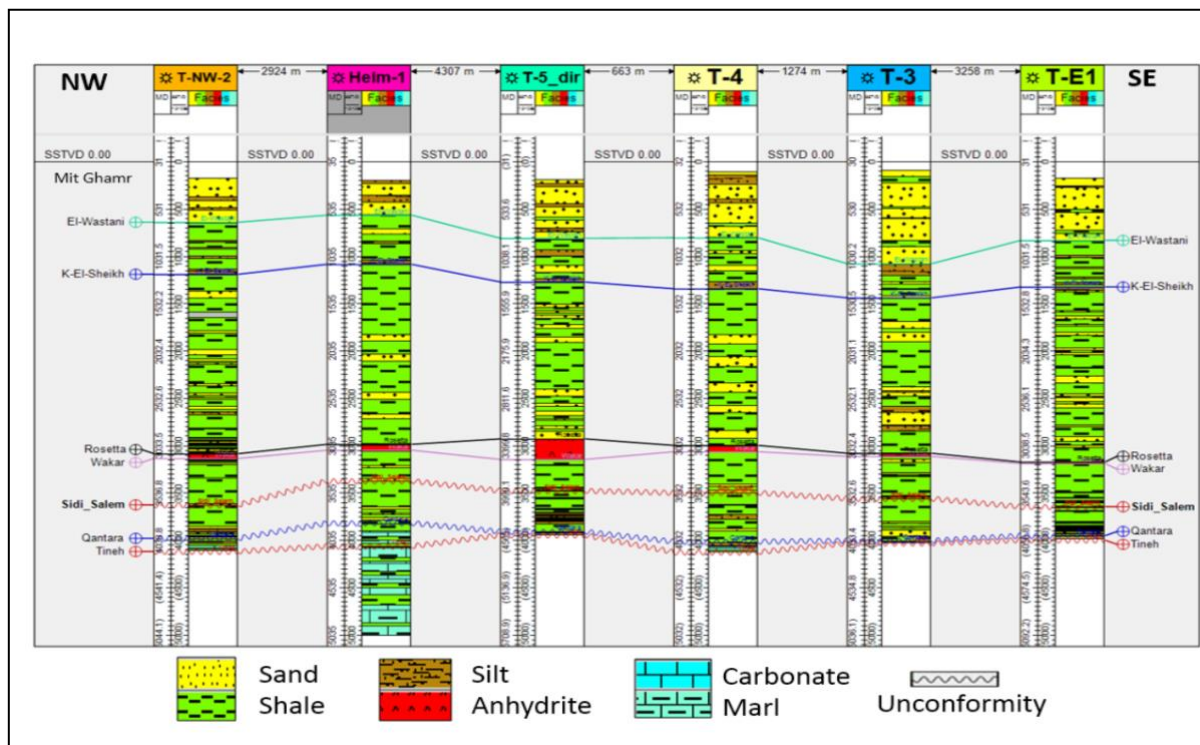

Fig. 3. Litho-statigraphic correlation of the studied well from the NW (Temsah-NW) to SE (Temsah) directions

3. Materials and Methods

The data used in the current study include well logs and composite mud logs from six wells; four from the Temsah field (T-3, T-4, T-5, and T-E1 wells) and two from the Temsah-NW field (H-1 and T-NW-2 wells). Geochemical analyses involved both TOC and Rock-eval pyrolysis analysis involved 49 ditch samples from T-4 well, representing the Temsah areas. The electric well-logs including gamma ray (GR), deep resistivity (ILD), sonic (DT), density (RHOB), and neutron (NPHI) are used to interpret the lithological compositions with mud logs according to the basis of well-logging interpretation (Rider, 2002).

The amounts of TOC (total organic carbon) for the wells lack geochemical analysis (T-2, T-3, T-E1, and T-NW-1) are measured according to the Δ-Log-R technique (Passey et al., 1990) based on sonic and deep resistivity logs as follows: Δ Log-R= log10 (LLD/R baseline) + 0.02 (ΔT/ ΔT baseline) Where; LLD: is the deep resistivity measured in ohm.m; ΔT: is the sonic measured in μ sec/ft.; R baseline= 2 ohms.m, ΔT baseline = 100 μ sec/ft.; Then the TOC is calculated from the following equation: TOC = (Δ Log-R) $\times$ 10 (2.297-0.1688 $\times$ LOM); LOM= 7 (it corresponds to the onset of maturity for oil-prone kerogen)

The ditch samples were pulverized to 0.420 mm and stirred in a beaker with 10% concentrated HCL for about one hour to remove any carbonate contents in the specimen. Further heating at 70°C applies to samples rich in carbonate and dolomites. Then the samples were washed and dried for the next geochemical analysis applied. A semi-quantitative analysis by combustion of 1 gm samples in an

oxidized medium using a Leco-crucible at approximately 1200ºC. The organic carbon that was converted to gases state measured its amounts by an infrared detector and sensor (Leco C230 system) and then measured organic carbon was calibrated to express as TOC (wt,%). SRA (source rock analyzer) instrument is used in pyrolysis techniques to measure a quantitative amount of released hydrocarbon during each stage of continuous sample heating (S_1, S_2) express as (mg HC/g rock) by FID. Tmax represents the threshold maximum peak of the S_2 curve. Whilst S_3 is the amount of CO_2 detected by the IR detector throughout the pyrolysis (mg CO_2/g rock).

Many parameters are used in the present study from rock-eval pyrolysis, including HI (hydrogen index) = S2/TOC ×100): it is used to characterize the origin and maturity of the kerogen. It is measured in milligrams of hydrocarbons per gram of TOC; OI (oxygen index) = S3/TOC ×100, it is measured in milligrams of hydrocarbons per gram of TOC; PI (Production index) = S1/ (S1+S2) it is used to indicate maturity state, how much of the organic matter is converted to hydrocarbons and Ro (vitrinite reflectance) calculated according to Ro_{cal}= (0.0317 × T_{max})- 13.224 (Lohr and Hackly, 2021); OSI (oil saturation index) = S1* 100/TOC). RHP (relative hydrocarbon potential) = (S1+S2)/TOC (Peng et al., 2019). Calculated Ro versus the depth relationship is established by regression chi-square exponential fit correlation coefficient using Origin Pro v.2014 software. Petromode software v11 was used to illustrate the burial history diagrams of the studied well T-4. All the geochemical analyses are done at laboratories of SCS (strato-chem-services), Cairo, Egypt.
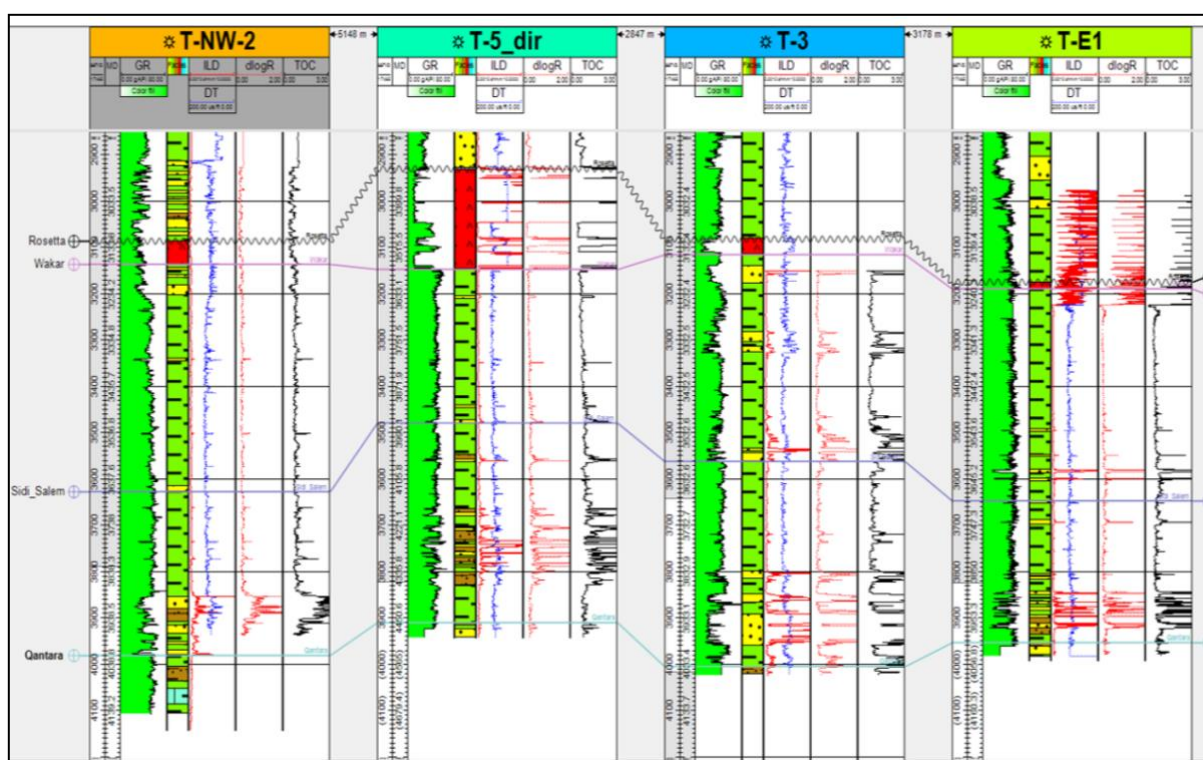
4. Results

The penetrated formations in the six studied boreholes is variable in thickness, from the base to the top, as shown in Fig. 3. The thickness of the Tineh Formation is not determined because the bottom depth is not recorded. Qantara Formation is recorded in Helm-1, T-NW-2, T-3, T-4, T-5, and T-E1 wells composed mainly of shale and carbonate. The vertical thickness of the Qantara Fm ranges from 28 to 246m, showing a maximum thickness toward the east than the west direction. Sidi Salem Formation is recorded in all studied wells and is composed of shale with sandstone and siltstone intercalation. The thickness of Sidi-Salem Fm ranges from 299 to 444 m. Wakar Fm is recorded in all wells and is composed of shale with sandstone intercalation. The thickness of Wakar Fm is variable and ranges from 323 to 491 m. The Miocene succession ends with a sequence of evaporites (Anhydrite) of Rosetta Fm with a strong variation in thicknesses from 5 to 67 m. Kafr El-Sheikh Fm is recorded in all studied wells with vertical huge thicknesses ranging from 1700 to 2163m composed of thick shale with sandstone and siltstone intercalations. El-Wastani Fm recorded in all studied wells range from 350 to 550m in thickness composed of shale with sandstone and intercalated siltstone. The sedimentary succession in all wells is capped by the Pleistocene Mit-Ghamr Fm which is composed of sandstones with thin siltstone intercalations.

The TOC and rock pyrolysis of TOC-rich interval depths ≥1 from depths of 3120m to 4140m in the studied well T-4 are summarized with the result of calculated rock pyrolysis parameters and calculated vitrinite reflectance in the measured intervals (Tables 1). TOC for other boreholes for which geochemical data are not available (T-NW-2, T-5, T-3, T-E1, and Helm-1) is determined from depth resistivity and sonic logs using the formula of Passey et al. (1990) (Fig. 4). TOC from log data shows a lower zone of high TOC in the lower part of the Qantara Fm. in all wells studied, two zones of high TOC in the middle part of the Sidi Salem Fm. in T-3 and T-5 that are absent in well T-NW-2, and a zone of high TOC in the Wakar Fm. in T-3 and T-5 that is absent in well T-NW-2 (Fig. 4).

Table 1. Rock-eval pyrolysis data and their calculated parameters of three penetrated Qantara, Sidi-Salem and Wakar   Fms, T-1 well, Temsah concession, east offshore Nile-Delta.

Age	Formations	Depth interval (m)	Thickness (m)	Total samples	Values	TOC (wt,%)	S_1 (mg HC/g rock)	S_2 (mg HC/g rock)	S_3 (mg CO$_2$/g rock)	GP=S_1+S_2 (mg HC/g rock)	S_2/S_3	HI (mg HC/ g TOC)	OI (mg CO$_2$/g TOC)	RHP= (S$_1$+S$_2$)/TOC	PI= S$_1$/(S$_1$+S$_2$)	OSI= (S$_1$/TOC) *100	Tmax (°C)	Vitrinite Reflectance (R%eal,%)
Late Miocene	Wakar	3120-3520	400	14	Min.	0.76	0.10	0.69	0.69	0.79	0.63	74	86	93.33	0.05	10.75	420	0.09
					Max.	1.27	0.30	3.18	1.53	2.91	2.86	250	138	263.78	0.28	35.29	434	0.53
					Average	1.02	0.18	1.76	1.17	1.90	1.46	162	112	179.91	0.11	17.50	428	0.33
Middle Miocene	Sidi – Salem	3550-3960	410	19	Min.	0.74	0.05	0.26	0.63	0.32	0.34	35	49	40	0.04	5.88	425	0.25
					Max.	1.56	0.33	5.31	1.88	5.51	5.43	466	177	483.49	0.16	20	446	0.91
					Average	1.13	0.16	2.64	1.11	2.81	2.26	209	101	222.93	0.08	13.51	434	0.52
Oligocene	Qantara	3990-4140	150	7	Min.	0.90	0.20	3.79	0.62	3.99	5.82	325	52	339.46	0.04	13.51	440	0.72
					Max.	2.05	0.47	9.45	1.08	6.76	8.75	458	69	484.62	0.06	26.92	458	1.29
					Average	1.52	0.33	6.26	0.85	6.04	6.98	405	59	426.59	0.05	21.72	446	0.92

Fig. 4. Illustrated measured results of TOC throughout Wakar, Sidi-Salem and Qantara Fms obtained from the resistivity and sonic logs in T-NW-2, T-5, T-3 and T-E1 boreholes

5. Discussion

5. 1. Quantities of OM in Investigated Boreholes

The amount of biomass preserved is a function of primary productivity. Many factors control the amount of OM preserved in sedimentary rock (Bjorlykke, 2010; El Atfy and Ghassal, 2022). As the amount of preserved OM increases the opportunity for sedimentary rock increases to be considered a source rock and vice versa. The geochemical quantitative measuring of the TOC in the examined rock is expressed in weight percentages, which refer to the quantity of the accumulated and preserved OM in any sedimentary strata (Tissot and Welte 1984; Edress and Abdel-Fatah, 2018; Hazra et al. (2017); Hunt, 2000). The maximum recorded measurement of TOC equal to 2.02wt.% was recorded within Qantara Fm of the T-4 well while the lowest average values were recorded related to Wakar Fm of T-4 well (Table 1). The 2-D distribution of TOC was illustrated in the present study for two formations of Wakar and Sid-Salem based on the accompanied TOC gathering values from both geochemistry and well-log calculation of wells without the geochemistry measurements, as shown in Figs. 4 and 5.
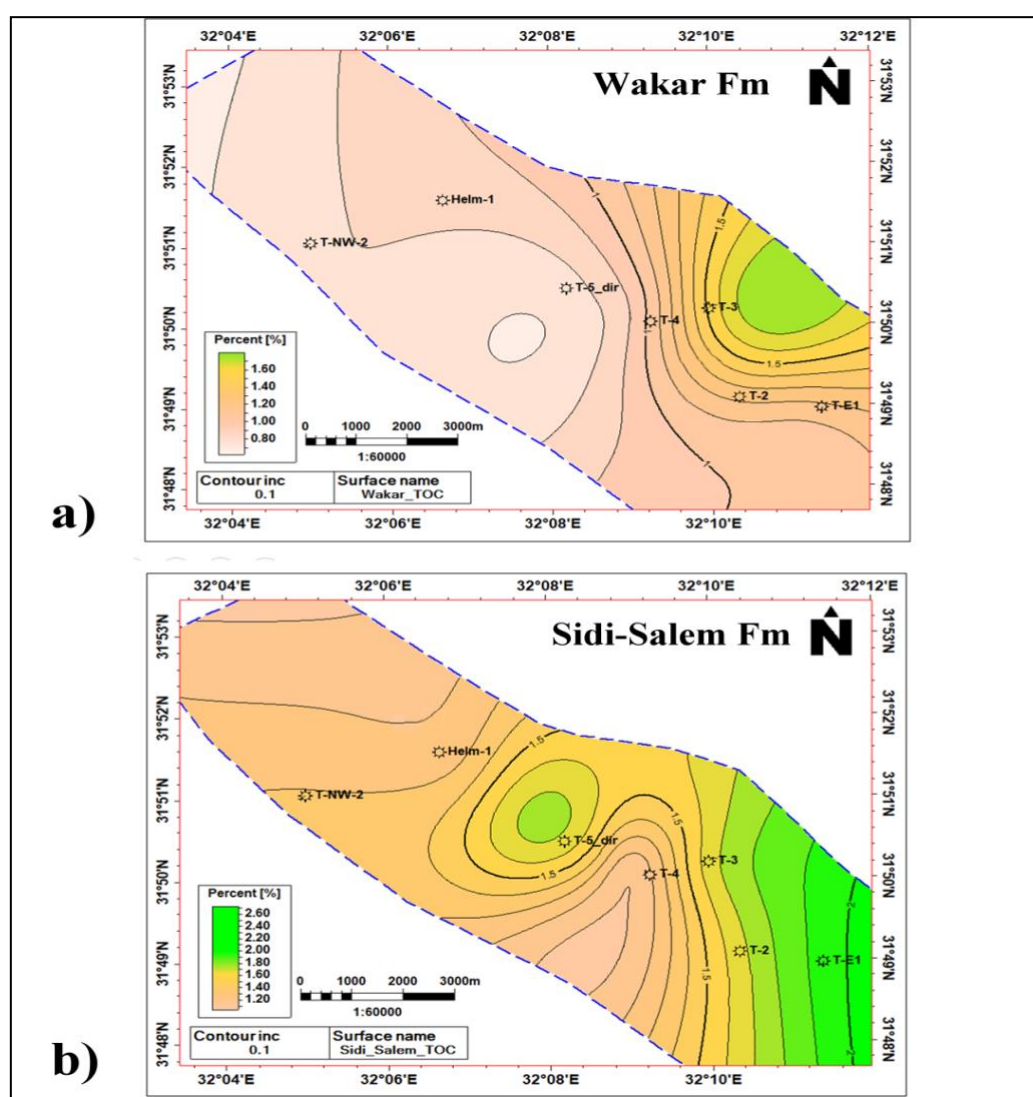

Fig. 5. 2-D TOC distribution maps of Wakar and Sidi-Salem Fms thorough the investigated Temsah and Temash-NW areas

The quantity of the OM was classified by Peters and Cassa (1994) into five categories according to their TOC amounts of poor OM bearing formation of TOC 0.5wt.%, fair of TOC (0.5-1wt.%), good of TOC (1-2wt.%), very good of TOC (2-4wt.%) and excellent exhibit much higher TOC > 4wt.%. The average TOC values of the investigated formations of Wakar (1.02wt.%), Sidi-Salem (1.13wt.%), Qantara (1.52wt.%), characterized good quantity of OM in the present studied wells.

As shown in Fig. 5, the Sidi-Salem Fm appears to be the richest in TOC than the Wakar Fm. The south-eastern and central area of (Temsah) is characterized by preserved a higher quantity of OM of the studied formations than the North-western area (Temsah-NW), which may attribute to the site of excellent anoxic-dysoxic accumulation and preservation of OM in these areas. That eastern trend of increasing in TOC may be synchronized by a high pale OM productivity associated with commonly well-preserved anoxic conditions than oxic ones (Edress and El-Moghazy, 2022; Taha and Edress, 2022).

Rock-eval pyrolysis also gives an investigation the potentialities of source rock based on both S_1 (free HC in Rock) and S_2 (HC generated by thermal cracking of kerogen during the pyrolysis). However, before applying the Rock-eval parameters and indices for many of examined analyses in the present study, the author used the OSI (oil saturated index) (S1/TOC)×100) suggested by Smith (1994) and Jarvie et al. (2001) to eliminate either the contamination or staining samples from indigenous HC. Jarvie et al. (2001) suggested the samples of OSI > 100 may consider contaminated (non-indigenous) samples and must be excluded from any further interpretation. The present studied samples recorded the highest value of OSI equal to 35.29 of Wakar Fm, which confirms the validity of all collected samples for further measurements and interpretation (Table 1).

Fowler et al. (2005) considered that the S_1 values of <0.5 mainly occupy the source rock of poor OM quantity. All the examined samples in the studied borehole have a S1 values less than 0.5 mg HC/g rock, which corresponds to poor quantity source rocks according to the previous author (Table 1).

The sedimentary source rock, which contains S_2 (generative potential) values of <2.5 mg HC/g rock is considered a poor source rock (Garry et al., 2016). While as the S_2 values increase, the source rock transforms from fair to excellent of S_2>20 mg HC/g rock (Peter and Cassa, 1994). Accordingly, all the recorded S_2 values of the studied T-4 borehole are ranging from poor (1.76 mg HC/g rock; Wakar), fair (2.64 mg HC/g rock; Sidi-Salem) and good (6.26 mg HC/g rock; Qantara) (Table. 1). Plotted of studied samples on the TOC versus (S2) diagram according to Peter and Cassa (1994) (Fig. 6) show that all represented formations in the studied formations have a poor-fair to good potential with of the T-4 well.
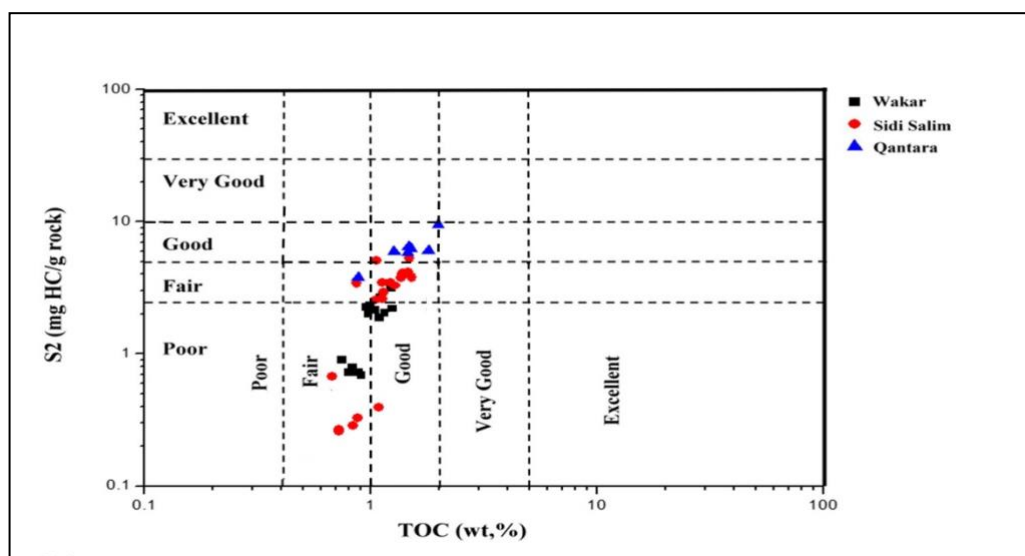

Fig. 6. Cross plot of S2 versus TOC for penetrated formations in T-4 borehole in the Temsah area

5.2. Types of Preserved OM

The HI (hydrogen index) plus the S_2/S_3 ratios can give a direct identification of the kerogen types involved in the studied formations (Waples, 1985). Peter and Cassa (1994) mentioned that the kerogen type-III mainly characterized by S_2/S_3 ratios <1 with HI <50, while the kerogen type-IV possessed an S_2/S_3 ratio range between 1-5 with HI ratio within the limits of 50-200mg HC/g rock. In the T-4 well, the studied formation shows a relative difference in OM types. The Wakar Fm in T-4 well has an S_2/S_3 ratio of 1.47 and HI of 162mg HC/g rock are belonging to kerogen type-III, whilst the Sidi-Salem and Qantara are belonging to kerogen types-II/III and II of S_2/S_3 ratios (2.26 and 6.98) with HI values equals (209 and 405mg HC/g rock) characterizing gas and oil-prone in respective order (Table 1).

The same previous conclusion was obtained by plotting all samples related to the T-4 borehole on the S2 versus TOC diagrams established by Delgado et al. (2018) (Fig. 7). Most of the T-4 borehole, the Wakar and Sidi-Salem Fms lay within types ranges from IV to III. While the Qantara samples occupy the area of type II kerogen. Parts of samples in related to T-4 well lay in organic lean area, which is characterized by a considerably low OM preservation and/or oxidation of TOC less than 1 (Fig. 7).
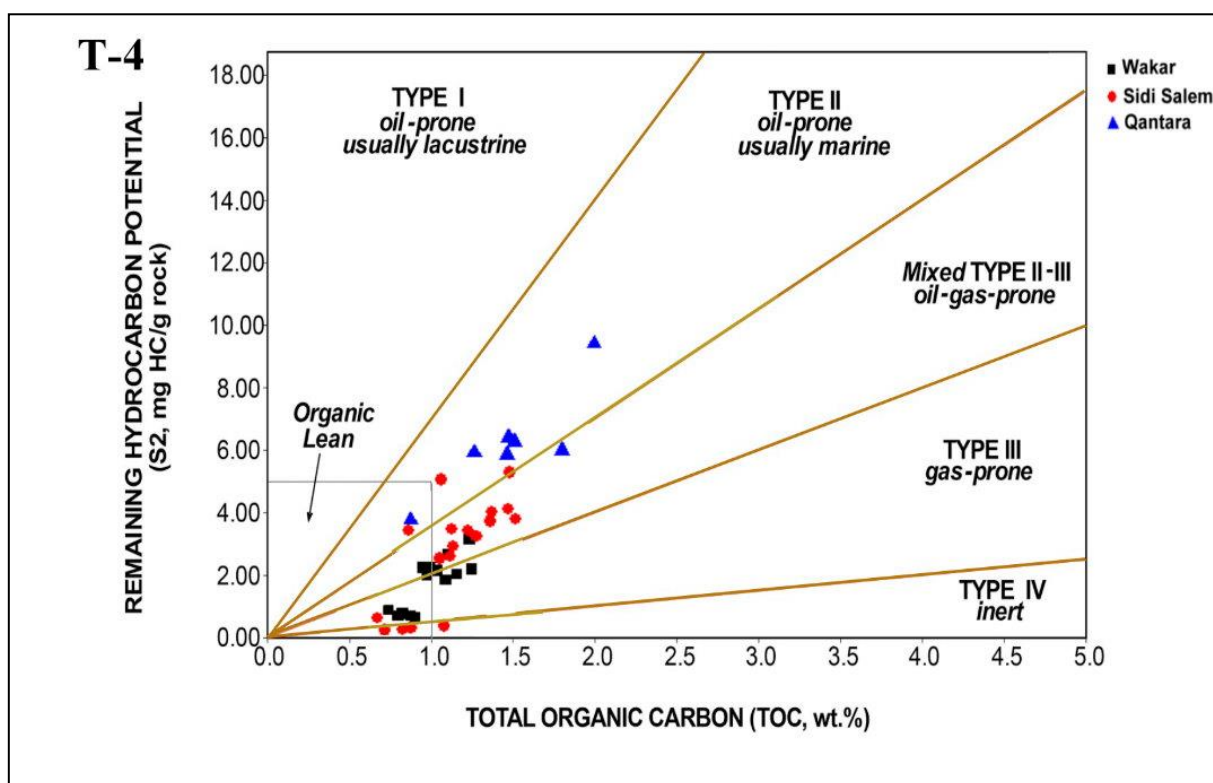

Fig. 7. Cross plot of the remaining hydrocarbon potential S2 against TOC for penetrated formations in T-4 borehole in the Temsah area

The types of HC productivity of the present studied boreholes samples are expressed by plotting samples' presentive formations on the HI against the TOC diagram according to Delvaux et al. (1990) (Fig. 8). Fig. 8 showing the T-4 samples beside gas-prone potentiality considerable parts of samples related to the Wakar and Sidi-Salem Fms belong to the fair-oil source. The samples represented the Qantara Fm within the same borehole showing another potentiality of a good oil source (Fig. 8).
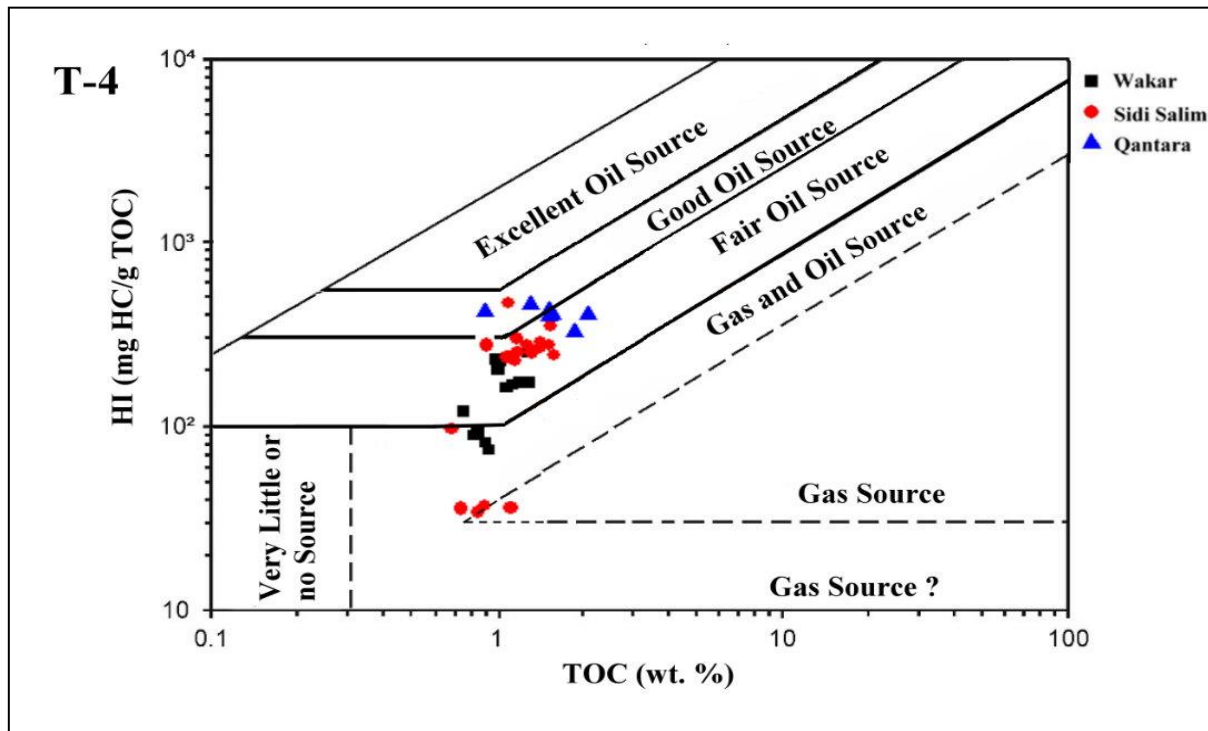
Fig. 8. Cross-plot of HI versus TOC according to Delvaux et al. (1990) showing the types of HC produced sources of investigated source rock penetrated formations in the T-4 borehole in the Temsah area

5.3. Maturity of the Preserved OM

R_o (random vitrinite reflectance), T_{max} and PI (production index) are commonly used as ideal parameters to distinguish the progress of OM maturity in any borehole-bearing strata (Hunt, 2000; Atta Peters et al. 2015; Hazra et al. 2017). Instead, the measured Ro the author used R_{ocal} (calculated vitrinite reflectance) according to the formula of Lohr and Hackly (2021) ($R_{ocal} = (0.0317* T_{max})-13.224$) to distiunguished the maturity level in the present studied well. The $_{Rocal}$ based on the previous formula shows that in the T-4 well, both Wakar and Sid-Salem Fms have average R_{ocal} values of 0.33 and 0.52 less than <0.6 belonging to the immature diagenesis stage of maturation, whilst the Qantara Fm show average R_{ocal} values of 0.92 characterizing the late-mature catagenesis stage of maturation according to maturity levels of both Tissot and Welte (1984) and Wust et al. (2012).

Plotted of the studied samples on the R_o versus TOC discrimination chart apply in the present study to determine the suggested values of SRI (source rock index) according to Pang et al. (2019). The logarithmic curved lines of the SRI were established by Pang et al. (2019) to determine the actual expelled HC compared to the promised HC expelling for optimal source rocks (Fig. 9). Most of the samples in the T-4 borehole included the Wakar and Sidi-Salem are concentrated in the same area of poor source rocks with few samples related to non-HC source rocks of SRI <zero. In the same T-4 borehole, most of the Qantara samples exceed the SRI line of 25, representing an intermediate actual expelling HC of medium source rock (Fig. 9).
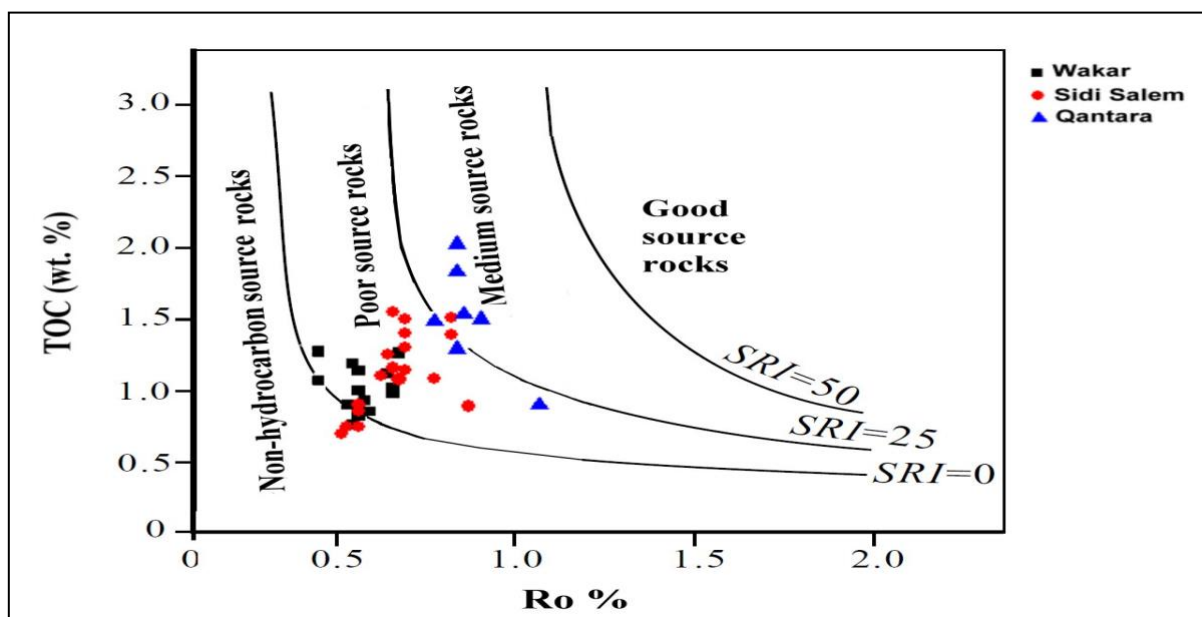
Fig. 9. Discrimination chart of TOC against Ro of studied samples determining the SRI values of each penetrated formations in T-4 borehole in the Temsah area according to Pang et al. (2019)

Plotted of the studied samples in the investigated boreholes (Helm-1 and T-4) on the Ghori and Haines (2007) and Delgado et al. (2018) Diagram as shown in Fig. 10 showing the Wakar Fm is not proceeding value of $T_{max}=435°C$ indicating immature stage, while nearly half of Sidi-Salem Fm samples occupy both of immature and mature oil-window stages. The entire samples of Qantara belong to the mature stage of the oil window in the T-4 well (Fig. 10).
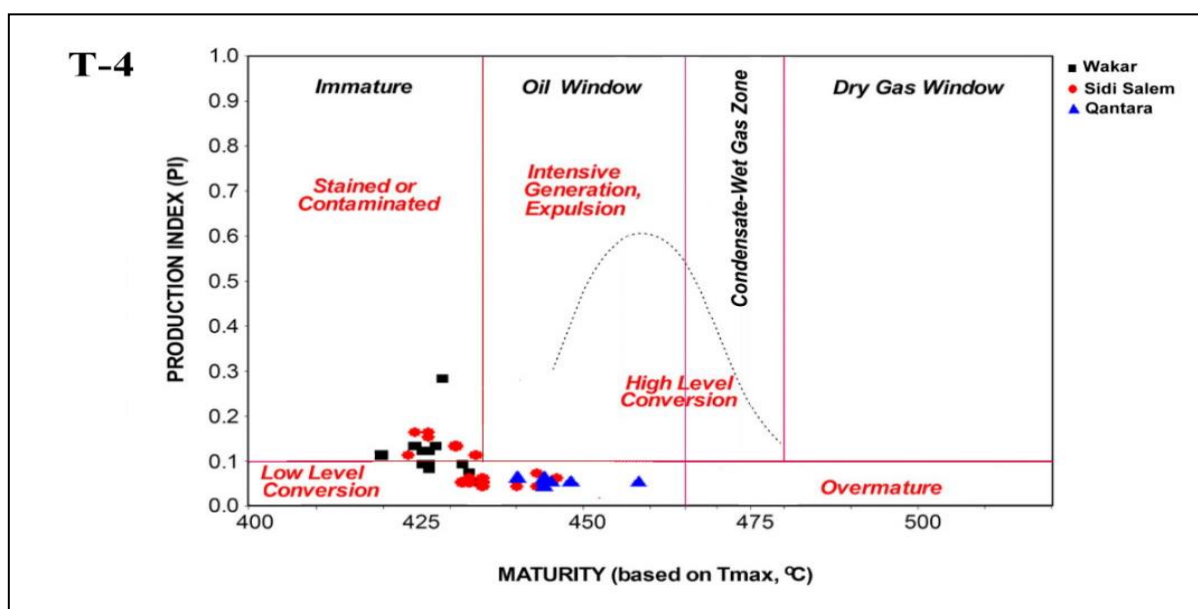

Fig. 10. Cross plot of PI against T_{max} of the penetrated formations in T-4 borehole in the Temsah area. According to Ghori and Haines (2007) and Delgado et al. (2018)

5.4. Expulsion Threshold, ASDL and Suggested Depths Of Maturity

Two methods are used to predict the maturity levels, Expulsion threshold and ASDL depths in the investigated T-4 borhole, taking into account the thermal maturity level changes from one type-kerogen to another according to the method established by Pang et al., 2019, Edress et al., 2021, Edress et al., 2022 (Fig. 11). Tissot and Welte (1994) and Al-Areeq (2018) measured the Ro, which characterized the different maturity levels concerning each kerogen type as follows; the Onset stage of oil generation is differentiated based on R_o as (0.65 for type-I; 0.5 for type II and 0.55 for type-III kerogens), while the stage of peak oil generation has R_o of 1.1 (type-1), 0.8 (type-II) and 0.9 (type-III). The stage of the end of oil generation is characterized by $R_o>1.4$ for all kerogen types.
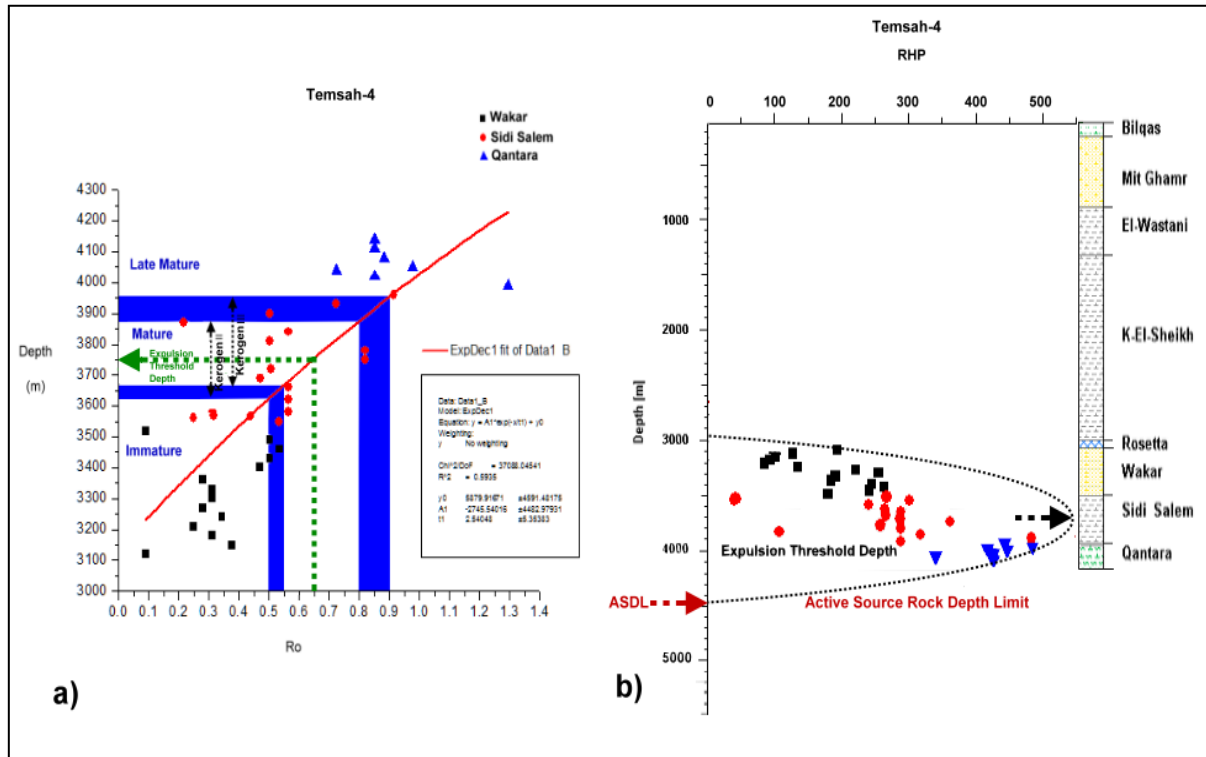

Fig. 11. a) Prediction of maturity level depths and expulsion threshold depth in T-4 well by using statistical exponential fit 1st order between the depth and R_o based on OM types according to Edress et al. (2021; 2022); b) another method used to predict the expulsion threshold and ASDL depths based on the maximum peak curve of the RHP values according to Pang et al. (2019)

Based on the previous identification of the kerogen types within the studied OM-bearing formations in the T-4 borehole. The statistical chi-square exponential fit applied for the studied samples between the depth against the Ro, identifies the depths of each maturity stage by methods of Edress et al. (2021 and 2022) as illustrated in Fig. 11. The measured expulsion threshold depth by these methods are recorded at a depth of 3750m in the T-4 borehole that fits the intersected lines of the R_o value of (0.65). From the above-mentioned results, the depth of 3950m is considered the limit between the immature (diagenesis) stage from the deeper mature (catagenesis) stage in the T-4 borehole.

By applying another method according to Pang et al. (2019) to determine the expulsion threshold depths in the studied well by showing the depth of the apex points represented the maximum curvature of the RHP values throughout the studied wells (Fig. 11). Moreover, the ASDL (active source rock depth limits) was distinguished by Pand et al. (2019) as a direct minimum retreat of the RHP values from the peak apex points by increasing depths. The expulsion threshold depth of HC generation within the T-4

borehole is recorded at a depth of 4450m (Fig. 11). The relatively shallowing of the expulsion threshold and ASDL depths in the T-4 borehole may attribute to the ancient geothermal gradient in the studied areas.

5. 5. Lithology Against OMRI and OMPI

Based on the previous results, it should consider the concept mentioned that not all the previously believed formations which contain sufficient organic matter are capable to be considered a source rock when thermal maturity is applied. To realize this concept, the author used the three-step method suggested by Edress et al. (2021) to distinguish the OMRIs in the studied well based on the previous results concerning the quantity, quality, and maturity parameters (Fig. 12).
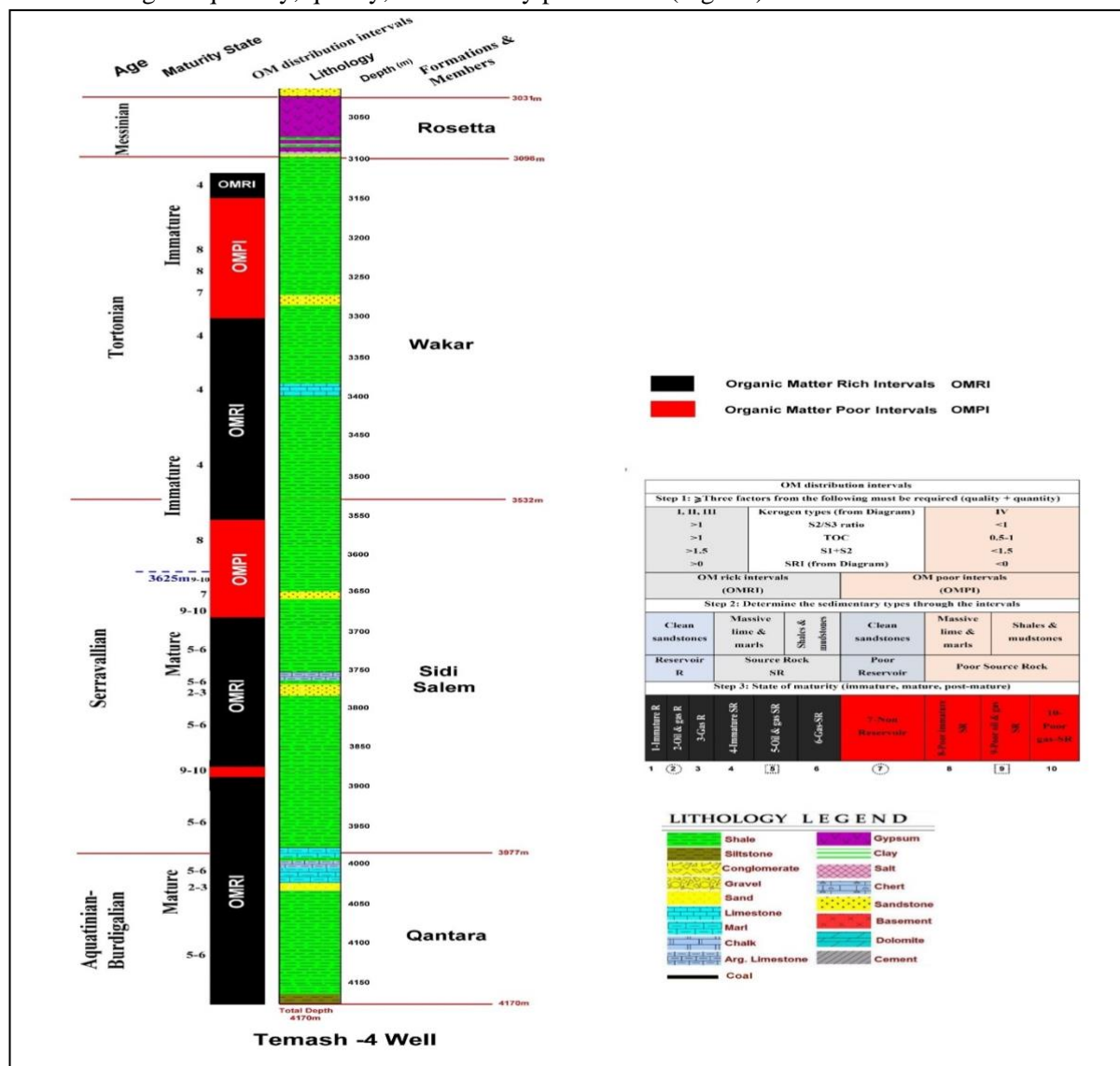

Fig. 12. Lithology against the OMRI and OMPI in the studied borehole representing the Temsah area according to Edress et al. (2021)

Geochemical analysis and lithological identities of the postulated OM-bearing formations in the investigated well distinguish a four-thick OMRI (organic matter-rich intervals) in T-4 borehole. The OMRI comprises 66.68% of the Wakar, 65.17% of Sidi-Salem and 100% of Qantara Fms in the T-4 well. They comprised intervals depths of 3120m-3150m and 3300m-3559.4m belonging to Wakar Fm, from 3580–3870m belonging to Sidi-Salem Fm and from 3977–4170 m belonging to Qantara

Formation. The geochemical data reveals that Wakar Fm in the T-4 well considers immature source rocks. While mature OMRI within Sidi-Salem and Qantara Fms in the T-4 well represented as an effective mature source rock.

Greatly observed notice as shown in Fig. 11, the T-4 well at the depth of 3780 m within the Sidi-Salem Fm and the depth of 4440 m within Qantara Fm show a reservoir character of sandstone pay zones.

5. 6. Burial History and Age of Maturation

The burial history models of the investigated geochemical studied borehole was illustrated according to Easy% Ro (Sweeney and Burnham 1990) (Fig. 13). Burial history of T-4 show that the Lower Qantara enter the early oil zone at 2.8Ma at a depth of 3800m. the Lower Sidi-Salem enter the same early oil window at 2.3Ma and Lower Wakar at 0.7Ma at depths of 3890m and 3420m, respectively. The Qantara enter the main oil zone at 1.8Ma at a depth of 4000m and the lower Sidi-Salem at 1.5Ma and did not proceed to the main oil zone yet.
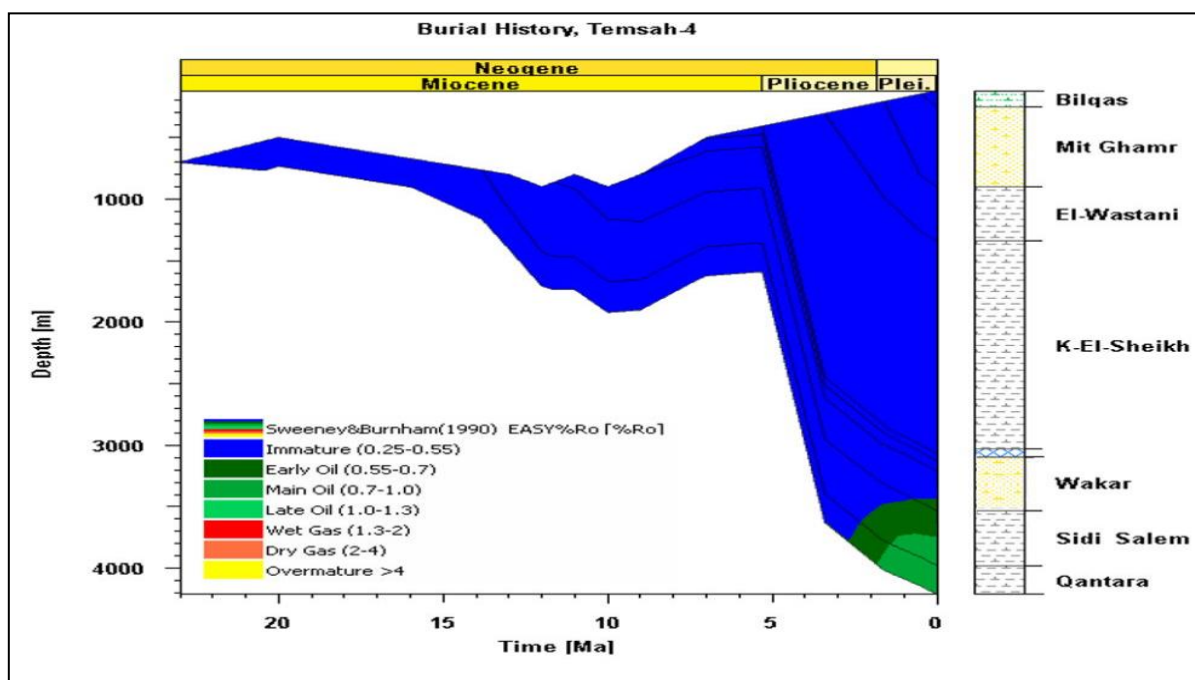

Fig. 13. Burial history of the penetrated formations in T-4 borehole in the Temsah area

6. Conclusions

Source rock evaluation of the Temsah and Temsah-NW concessions in the offshore Nile Delta recognizes varieties of different quantity, quality and maturity levels of the boreholes penetrating formations of Qantara, Sidi-Salem and Wakar from the Rupelian to Tortonian periods. The geochemical analysis combined with the types of sedimentary succession throughout the T-4 (Temsah-4), recognized relatively four thick organic matter-rich intervals (OMRI) in T-4 well comprising Wakar Fm (30m) and (259.4m), Sidi-Salem Fm (290m) and Qantara Fm (193m). They represent 66.68% of the entire Wakar, 65.17% of the entire Sidi-Salem and 100% of the entire Qantara thickness. These facts spotlight the conclusion that not all thicknesses of previously believed source rock-bearing formations are acceptable to assign as source rocks. Just OMRI within any formation may be acceptable to consider source rocks than the other OMPI. The OMRI in the present studied borehole shows zones of either immature source rock intervals involved (Wakar Fm in the T-4 well) or effective mature source rock intervals of Sidi-Salem and Qantara Fms in the T-4 well. The 2D illustrated maps of the measured and calculated TOC

throughout the studied boreholes reveal a trend of OM richness eastward from the Temsah-NW to the Temsah areas. Besides the recorded types II and II/III Kerogen-bearing Fms of the Temash area indicate the origin of marine oil-prone source rock than terrestrial gas-prone sources. Expulsion threshold depths of HC generation within the Temsah area were recorded at a depth of 3700m, that depth coincides with the depth of the peak of oil windows that are equivalent to R_o (0.65) in the studied well. The age of 2.8Ma is the time of early hydrocarbon generation stages where the base of Qantara Fm enters the early mature stage at the T-4 well. The maturity continues to most of Sidi-Salem Fms in the T-4 well.

Acknowledgements

References

Al Areeq, N.M., 2018. Characterization and Hydrocarbon Petroleum Source Rocks Generation, chapter 1, INTECH open science, 1-30.

Atta Peters, D., Achaegakwo, C.A., Garrey, P., 2015. Palynofacies, organic geochemical analyses and hydrocarbon potential of the Takoradi 11-1 Well, Saltpond basin, Ghana. Petroleum and Coal, 57(5), 478-499.

Bertello, F., Barsoum, K., Dalla, S., Guessarian, S., 1996. Temsah discovery: a major gas field in a deep sea turbidite environment. EGPC, 13th Petrol Exploration Prodduction Conf. Cairo 1, 165–180

Bjorlykke, K., 2010. Petroleum geoscience from sedimentary environments to rock physics, Springer-Verlag Berlin Heidelberg 2010. 508.

Delgado, L., Batezelli,A., Luna, J., 2018. Petroleum geochemical characterization of Albian Oligocene sequences in the Campos Basin: Case study: Eastern Marlim oil field, offshore, Brazil Journal of South American Earth Science, 88, 715-735.

Delvaux, D., Martin, H., Leplat, P., Paulet, J., 1990. Geochemical characterization of sedimentary organic matter by means of pyrolysis kinetic. In: Durand, B, & Behar, F., editors. Advances in organic geochemistry 1989. 16. Pergamon, Oxford: Organic Geochemistry; 1990. 175–87.

Dolson, J., 2020. The Petroleum geology of Egypt and history of exploration. in: Hamimi Z., El-Barkooky A.,

Martínez Frías J., Fritz H., Abd El-Rahman Y. (eds) The Geology of Egypt. Regional Geology Reviews. Springer, Cham.

Dolson, C.J., 2016. Understanding oil and gas shows and seals in the search for hydrocarbons. Springer International Publishing Switzerland, Switzerland.

Garry, P., Atta Peters, D., Achaegakwo, C., 2016. Source-Rock potential of the Lower Cretaceous sediments in SD-1X WELL, Offshore Tano Basin, South Western Ghana, Petroleum and Coal, 58(4): 476-489.

El Atfy, H., Ghassal, I., 2022. Advances in petroleum source rock characterizations: Integrated methods and case studies. Springer.

El-Moghazy, A F. Deaf, A. S.. Edress, N. A.A.., 2023. Integrated organic, inorganic geochemical and palynofacies analyses to characterize the paleoenvironment of the Tortonian (Late Miocene) Wakar Formation, offshore Nile Delta, Egypt, Marine and Petroleum Geology, 156, 106456.

Edress, N.A.A., Abdel-Fatah, A.R., 2018. Fuel analyses and rank determination of the Egyptian Maghara main Coal seam, north central Sinai, Egypt, Egyptian Journal of Petroleum, 27(4), 477-484.

Edress, N.A.A., Darwish, S., Ismail, A., 2021. Geochemical characterization of the source rock intervals, Beni-SuefBasin, West Nile Valley, Egypt. Open Geosciences, 13(1), 1536-1551.

Edress, N.A.A., El-Moghazy, A.F., 2022. Geochemical and organic petrographic analyses on the Late Eocene

bentonitic shale bed in Kom Aushim vicinity, Fayum, Egypt; Paleoenvironmental implications, Journal of African Earth Sciences, 195, 104647.

Edress, N.A.A., Fagelnour, M.S., Hassan, M.H.M., 2022. Subsurface geology and geochemical evaluation of the

Middle Jurassic-Lower Cretaceous organic-rich intervals, West Kalabsha area, Western Desert, Egypt. Arab Journal of Geosciences 15, 1401 (2022).

Edress, N.A.A., Fagelnour, M.S., Mahmoud, A.A., 2022. Petrographic and organic geochemical studies of the Oligocene-Pliocene mud-rich formations, East Mediterranean concession, Egypt. Arabian Journal of Geosciences 15, 1528.

El Heiny, I., Enani, N., 1996. Regional stratigraphic interpretation pattern of Neogene sediments, Northern Nile Delta, Egypt, E.G.P.C. 13th Exploration and Production Conference, 1, 270–290

Fowler, M., Snowdon, L., Stasiuk, V. 2005. Applying petroleum geochemistry to hydrocarbon exploration and exploitation. American Association of Petroleum Geologists Short Course Notes, Calgary, Alberta.

Ghori, K.A.R., Haines, P.W., 2007. Paleozoic Petroleum Systems of the Canning Basin, Western Australia: A review. Search and Discovery Article, 10120.

Hazra, B., Dutta, S., Kumar. S., 2017. TOC calculation of organic matter rich sediments using Rock-Eval pyrolysis: Critical consideration and insights Inter. Journal of Coal Geology .169:106-115

Hanafy, S., Nimmagadda, S.L., Mahmoud, S.F., Mabrouk, W.M., 2016. Regional integrated interpretation of the hydrocarbon prospectivity of the Nile Delta, Offshore Egypt. Arabian Journal of Geosciences, *9*(376),1-18.

Hemdan, K., El Alfy, M., Enani, N., Barrasi, M., Monir, M., 2002. Structural complexity of Pliocene and its impact on trapping mechanism, N. Port Said Concession, Egypt. Mediterranean Offshore Conference. (MOC, 2002).

Hunt, J.M., 2000. Petroleum Geochemistry and Geology, 2nd Eds. W. H. Freeman and Company.

Ismail, A., Ewida, H.F., Nazeri, S., Al-Ibiary, M.G., Zollo, A., 2022. Gas channels and chimneys prediction using artificial neural networks and multi-seismic attributes, offshore West Nile Delta, Egypt. Journal of Petroleum Science and Engineering, 208, 109349.

Ismail, A., Ewida, H.F., Al-Ibiary, M.G., Nazeri, S., Salama, N.S., Gammaldi, S., Zollo, A., 2021. The detection of

deep seafloor pockmarks, gas chimneys, and associated features with seafloor seeps using seismic attributes in the West offshore Nile Delta, Egypt. Exploration Geophysics, 52(4), 388-408.

Ismail, A., Ewida, H.F., Al-Ibiary, M.G., Gammaldi, S., Zollo, A., 2020. Identification of gas zones and chimneys using seismic attributes analysis at the Scarab field, offshore, Nile Delta, Egypt. Petroleum Research, 5(1), 59-69.

Jarvie, D.M., Morelos, A., Han, Z., 2001. Detection of pay zones and pay quality. Gulf of Mexico: application of geochemical techniques. Gulf Coast Association of Geological Societies Transactions*,* 51, 151-160.

Khaled, K.A., Attia, G.M., Metwalli, F., Fagelnour, M.S., 2014. Subsurface geology and petroleum system in the eastern offshore area, Nile Delta, Egypt. Journal of Applied Science Research*,* 4, 254-270.

Lashin, A., Abd El Aal, M., 2005. Contribution of AVO and multi attribute analysis in delineating the fluid content and rock properties of the gas-bearing reservoirs in the Northeastern part of Nile Delta, Egypt. Journal of Applied Geophysics, 4(2), 279-301.

Leila, M., Moscariello, A., 2018. Depositional and petrophysical controls on the volumes of hydrocarbons trapped in the Messinian reservoirs, onshore Nile Delta, Egypt, 4, 250–267

Lohr, C.D., Hackley, P.C., 2021. Relating Tmax and hydrogen index to vitinite and solid bitumen reflectance in hydrous pyrolysis residues: comparisons to natural thermal indices. International Journal of Coal Geology (Int J Coal Geol) 242,103768.

Marten, R., Shann, M., Mika, J., Rothe, S., Quist, Y., 2004. Seismic challenges of developing the pre-Pliocene Akhen Field offshore Nile Delta. The Leading Edge, 23(4), 314-320.

Nabawy, B.S., Shehata, A.M., 2015. Integrated petrophysical and geological characterization for the Sidi Salem-Wakar sandstones, off-shore Nile Delta, Egypt. Journal of African Earth Sciences, 110, 160-175.

Pang, X., Jia, C., Zhang, K., Li, M., Wang, Y., Peng, J., 2019. The depth limit for the formation and occurrence of fossil fuel resources. Earth Syst Sci Data Discuss. 72,1-26.

Passey, Q.R., Creaney, S., Kulla, J.B., Moretti, F.J., Stroud, J.D., 1990. A practical model for organic richness from porosity and resistivity logs: American Association of Petroleum Geologists Bulletin, 74(12), 1777–1794.

Peters, K.E., Cassa, M.R., 1994. Applied source rock geochemistry. In: Magoonand, L. B., Dow, W. G., (Eds.) The petroleum system from source to trap. American Association of Petroleum Geologists (AAPG,) 93-120.

Pigott, J.D., Williams, M.T., Abdel-Fattah, M., Pigott, K.L., 2014. The Messinian Mediterranean crisis: A model for the Permian Delaware Basin? In: Paper presented at the American Association of Petroleum Geologists (AAPG) international conference and exhibition, Istanbul, Turkey

Rider, M.H., 2002. The Geological interpretation of well logs, 2nd edition, Whittles Publishing. 280

Said, R., 1990. The Geology of Egypt 1. A. A. Balkema Publishers, Rotterdam, The Netherlands.

Shaaban, F., Lutz, R., Littke, R., Bueker, C., Odisho, K., 2006. Source-rock evaluation and basin modeling in NE Egypt (NE Nile Delta and northern Sinai). Journal of Petroleum Geology, 29 (2), 103-124.

Schlumberger, 1984. Well evaluation conference, Egypt. Schlumberger Middle East S. A.

Schlumberger, 1995. Well evaluation conference, Egypt. EGPC Report.

Smith, J.T., 1994. Petroleum system logic as an exploration tool in frontier setting, in Magoon, L.P., and Dow, W.G. (eds.), The petroleum system from source to trap. American Association of Petroleum Geologists (AAPG) Memoir, 60, 25-49.

Sweeney, J.J., Burnham, A.K., 1990. Evaluation of a simple model of vitrinite reflectance based on chemical kinetics. American Association of Petroleum Geologists Bulletin, 1990, 74: 1559-1570.

Taha, M.M.N., Edress, N.A.A., 2022. The role of geochemical and coal petrographic analyses to determine the depositional sets of Visean coal and shale sequence in Um Thora-Abu Hish area, Central Sinai, Egypt, Journal of African Earth Sciences, 196, 104716.

Tissot, B.P., Welte, D.H., 1984. Petroleum Formation and Occurrence. 2nd ed. Berlin: Springer, 148-180.

Waples, D.W. 1985. Geochemistry in petroleum exploration. International Human Resources and Development Corporation, Boston, 226.

Wust, R., Hackley, P., Nassichuk, B., Willment, N., Brezovski, R., 2012. Vitrinite reflectance versus pyrolysis Tmax data: Assessing thermal maturity in shale plays with spectral reflectance to the Duvernay shale play of Western Canadian sedimentary basin. Society of Petroleum Engineers, 167031, 1-11.

Younes, M.A., 2015. Natural Gas Geochemistry in the offshore Nile Delta, Egypt., chapter 2, 27-40. INTECH open science.